JCI The Journal of Clinical Investigation

$G\alpha_{12}$ ablation exacerbates liver steatosis and obesity by suppressing USP22/SIRT1-regulated mitochondrial respiration

Tae Hyun Kim, … , Cheol Soo Choi, Sang Geon Kim

J Clin Invest. 2018. https://doi.org/10.1172/JCI97831.

Research In-Press Preview **Hepatology** **Metabolism**

Non-alcoholic fatty liver disease (NAFLD) arises from mitochondrial dysfunction under sustained imbalance between energy intake and expenditure, but the underlying mechanisms controlling mitochondrial respiration have not been entirely understood. Heterotrimeric G proteins converge signals from activated GPCRs, and modulate cell signaling pathways to maintain metabolic homeostasis. Here, we investigated the regulatory role of $G\alpha_{12}$ on hepatic lipid metabolism and whole-body energy expenditure in mice. Fasting increased $G\alpha_{12}$ level in mouse liver. $G\alpha_{12}$ ablation markedly augmented fasting-induced hepatic fat accumulation. cDNA microarray analysis from *Gna12* KO liver revealed that $G\alpha_{12}$ signaling pathway regulated sirtuin 1 (SIRT1) and PPARα responsible for mitochondrial respiration. Defective induction of SIRT1 upon fasting was observed in the liver of *Gna12* KO mice, which was reversed by lentivirus-mediated $G\alpha_{12}$ overexpression in hepatocytes. Mechanistically, $G\alpha_{12}$ stabilized SIRT1 protein through transcriptional induction of USP22 via HIF-1α increase. $G\alpha_{12}$ levels were markedly diminished in liver biopsies from NAFLD patients. Consistently, *Gna12* KO mice fed high-fat diet displayed greater susceptibility to diet-induced liver steatosis and obesity due to decrease in energy expenditure. Our results demonstrate that $G\alpha_{12}$ regulates SIRT1-dependent mitochondrial respiration through HIF-1α-dependent USP22 induction, identifying $G\alpha_{12}$ as an upstream molecule that contributes to the regulation of mitochondrial energy expenditure.

$G\alpha_{12}$ ablation exacerbates liver steatosis and obesity by suppressing USP22/SIRT1-regulated mitochondrial respiration

Tae Hyun Kim,[1,¶] Yoon Mee Yang,[1,2,¶] Chang Yeob Han,[1,3] Ja Hyun Koo,[1] Hyunhee Oh,[4] Su Sung Kim,[4] Byoung Hoon You,[5] Young Hee Choi,[5] Tae-Sik Park,[6] Chang Ho Lee,[7] Hitoshi Kurose,[8] Mazen Noureddin,[9] Ekihiro Seki,[2] Yu-Jui Yvonne Wan,[10] Cheol Soo Choi,[4,11] and Sang Geon Kim[1,]*

[1]College of Pharmacy and Research Institute of Pharmaceutical Sciences, Seoul National University, Seoul 08826, Korea;

[2]Division of Digestive and Liver Diseases, Department of Medicine, Cedars-Sinai Medical Center, Los Angeles, California, 90048, USA;

[3]Department of Pharmacology, School of Medicine, Wonkwang University, Iksan, Jeonbuk, Korea;

[4]Korea Mouse Metabolic Phenotyping Center, Lee Gil Ya Cancer and Diabetes Institute, Gachon University of Medicine and Science, Incheon 21999, Korea;

[5]College of Pharmacy, Dongguk University, 32 Dongguk-ro, Ilsan dong-gu, Goyang, Gyeoggi-do 410-820, Korea;

[6]Department of Life Science, Gachon University, Seongnam, Gyeonggi-Do 461-701, Korea;

[7]College of Medicine, Hanyang University, Seoul 133-791, Korea;

[8]Department of Pharmacology and Toxicology, Graduate School of Pharmaceutical Sciences, Kyushu University, Fukuoka 812-8582, Japan;

[9]Fatty Liver Disease Program, Division of Digestive and Liver Diseases, Department of Medicine, Comprehensive Transplant Center, Cedars-Sinai Medical Center, Los Angeles, California, 90048, USA;

[10]Department of Medical Pathology and Laboratory Medicine, University of California, Davis, Sacramento, CA 95817, USA;

[11]Endocrinology, Internal Medicine, Gachon University Gil Medical Center, Incheon 21565, Korea

¶These authors contributed equally to this work.

*Contact information (Corresponding Author)

Sang Geon Kim, Ph.D., College of Pharmacy, Seoul National University, 1 Gwanak-ro, Gwanak-gu, Seoul 08826, Korea. Tel: +82-2-880-7840 Fax: +82-2-872-1795. E-mail: sgk@snu.ac.kr.

Conflict of interest statement: The authors have declared that no conflict of interest exists.

Abstract

Non-alcoholic fatty liver disease (NAFLD) arises from mitochondrial dysfunction under sustained imbalance between energy intake and expenditure, but the underlying mechanisms controlling mitochondrial respiration have not been entirely understood. Heterotrimeric G proteins converge signals from activated GPCRs, and modulate cell signaling pathways to maintain metabolic homeostasis. Here, we investigated the regulatory role of $G\alpha_{12}$ on hepatic lipid metabolism and whole-body energy expenditure in mice. Fasting increased $G\alpha_{12}$ level in mouse liver. $G\alpha_{12}$ ablation markedly augmented fasting-induced hepatic fat accumulation. cDNA microarray analysis from *Gna12* KO liver revealed that $G\alpha_{12}$ signaling pathway regulated sirtuin 1 (SIRT1) and PPARα responsible for mitochondrial respiration. Defective induction of SIRT1 upon fasting was observed in the liver of *Gna12* KO mice, which was reversed by lentivirus-mediated $G\alpha_{12}$ overexpression in hepatocytes. Mechanistically, $G\alpha_{12}$ stabilized SIRT1 protein through transcriptional induction of USP22 via HIF-1α increase. $G\alpha_{12}$ levels were markedly diminished in liver biopsies from NAFLD patients. Consistently, *Gna12* KO mice fed high-fat diet displayed greater susceptibility to diet-induced liver steatosis and obesity due to decrease in energy expenditure. Our results demonstrate that $G\alpha_{12}$ regulates SIRT1-dependent mitochondrial respiration through HIF-1α-dependent USP22 induction, identifying $G\alpha_{12}$ as an upstream molecule that contributes to the regulation of mitochondrial energy expenditure.

Introduction

The liver plays a major role in maintaining whole-body energy balance by regulating lipid metabolism (1, 2). Upon changes in nutrient availability following food intake, hepatic lipid metabolism is tightly controlled through fine-tuning regulation of both fatty acid (FA) oxidation and lipogenesis, which is an essential process for the maintenance of metabolic homeostasis under physiological and pathological conditions. When this equilibrium is disturbed by excess caloric supply and impaired energy expenditure due to mitochondrial dysfunction, ectopic lipid is accumulated within hepatocytes, favoring hepatic steatosis as an early risk factor for the development of non-alcoholic fatty liver disease (NAFLD) (2-4).

Both prolonged fasting and western dietary intake share the common metabolic feature in terms of increased concentrations of FA serving as a major fuel source. In the liver under starvation conditions, where the glycogen stores are depleted with the inhibition of lipogenesis, FAs mobilized from adipose tissues are oxidized primarily in mitochondria to produce ketone bodies and/or re-esterified into triglyceride (TG) for storage. In contrast, impaired mitochondrial FA oxidation in the liver is frequently observed along with increased de novo synthesis of FA in pathologic situations such as insulin resistance and obesity, indicating that mitochondrial capacity to oxidize FA plays a key role in modulating lipid metabolism. Thus, identification of the signaling node(s) regulating mitochondrial FA oxidation is warranted for the treatment of NAFLD. However, the pathways that control mitochondrial FA utilization in response to varying physiologic conditions are not entirely defined yet.

G proteins represent major molecular switches that converge varying cell surface signals from activated GPCRs upon diverse extracellular stimuli. Over 800 different genes encode GPCRs in humans, whereas only ~20 genes encode G proteins, implying a converging role of G proteins for signal transduction. The G protein α subunit, a component of heterotrimeric G proteins, can be classified largely into G_s, $G_{i/o}$, G_q, and G_{12}. Although the roles of G_s, $G_{i/o}$ and G_q have been well-characterized, G_{12} family members were identified relatively recently, and their functions have been uncovered with a slower pace (5). $G\alpha_{12}$ is ubiquitously expressed in metabolic organs including the

liver (6). In particular, $G\alpha_{12}$ has drawn considerable interests in the field of cancer biology due to its triggering effect on cell growth and oncogenic transformation (7, 8). Moreover, $G\alpha_{12}$ was overexpressed in highly proliferating cancer cells (8-11). Interestingly, a considerable portion of endogenous $G\alpha_{12}$, but not other $G\alpha$ subunits, is physically associated with mitochondria (12), raising the possibility that $G\alpha_{12}$ is associated with mitochondrial function (e.g., mitochondrial energy metabolism) more directly than other $G\alpha$ proteins. Given that mitochondrial activity favors cancer cell growth (13), it is presumed that $G\alpha_{12}$ may also contribute to energy metabolism in normal cells under pathophysiological conditions. However, the metabolic impact of $G\alpha_{12}$ signaling in cellular energy balance remained unexplored although recent studies have investigated the roles of a few other G proteins in lipid and/or glucose metabolism.

Sirtuin 1 (SIRT1), a NAD^+-dependent protein deacetylase, plays a role in the regulation of transcriptional network in various metabolic processes, especially FA oxidation (14, 15). However, the upstream regulator linking cell surface signaling and SIRT1 is incompletely understood. In the present study, cDNA microarray analysis using liver of *Gna12* knockout (*Gna12* KO) mice enabled us to define SIRT1, PPARα, and PPARγ-coactivator 1α (PGC1α) as the 'core partners' for the regulation of genes responsible for mitochondrial respiration controlled by $G\alpha_{12}$; Ablation or knockdown of $G\alpha_{12}$ gene suppressed SIRT1 induction by fasting, and its downstream mitochondrial target genes associated with FA oxidation. Consistently, *Gna12* KO mice subjected to fasting showed increased TG accumulation in the liver compared to WT mice, and this change was normalized by hepatocyte-specific $G\alpha_{12}$ overexpression. Mechanistically, we revealed that $G\alpha_{12}$ promotes SIRT1 stability by inducing ubiquitin-specific peptidase 22 (USP22) through hypoxia-inducible factor 1 alpha (HIF-1α), unraveling the novel regulatory role of $G\alpha_{12}$ in SIRT1 expression. Furthermore, we found that high-fat diet (HFD)-fed *Gna12* KO mice were prone to hepatic steatosis and obesity due to decrease in energy expenditure. In line with this, we observed that $G\alpha_{12}$ levels were markedly diminished in patients with either simple steatosis or non-alcoholic steatohepatitis (NASH) as compared to individuals without

steatosis. Our findings show that $G\alpha_{12}$ signaling controls lipid metabolism through the regulation of HIF-1α-USP22-SIRT1 axis, revealing its regulatory role in energy expenditure.

Results

Ablation of Gna12 augments fasting-induced liver steatosis in mice

Sustained fasting condition promotes liver steatosis as FA derived mainly from adipose tissue are being accumulated (16). To investigate whether $G\alpha_{12}$ level changes depending on nutritional status, we first assessed the effect of fasting on $G\alpha_{12}$ in mouse liver. Of note, fasting of WT mice for 24-48 h markedly enhanced $G\alpha_{12}$ expression in the liver (Figure 1, A and B), suggestive of the role of $G\alpha_{12}$ signaling in lipid metabolism. To better understand the metabolic impact of $G\alpha_{12}$ on the physiological adaptation to fasting, we then analyzed the lipid profiles in the liver of *Gna12* KO mice subjected to fasting for 24 h. *Gna12* KO mice displayed a significant increase in liver fat accumulation compared to WT mice as revealed by both histochemical and biochemical analyses for lipids (Figure 1, C-E). In contrast, serum TG and cholesterol levels were lower in fasted $G\alpha_{12}$KO mice presumably due to diminished fat secretion from hepatocytes (Figure 1F). Referring to the published literature, the distribution of genotypes from offspring of $Gna12^{+/-}$ intercrosses was Mendelian, and mice with either heterozygous or homozygous deletion of *Gna12* were fertile without apparent morphological or behavioral abnormalities (17). In order to provide insights into the physiological relevance of $G\alpha_{12}$ signaling pathway in our experimental model, male mice heterozygous for *Gna12* deficiency (*Gna12* Het mice) (Supplemental Figure 1A) were additionally subjected to fasting for 24 h together with WT and *Gna12* KO mice to compare hepatic lipid profiles between genotypes. As expected, the partial effect of heterozygous deletion of *Gna12* was corroborated in the context of hepatic lipid metabolism as assessed by Oil Red O staining of liver sections and triglyceride measurements (Supplemental Figure 1B). These results indicate that $G\alpha_{12}$ signaling may be adaptively increased under fasting condition, whereas a deficiency in $G\alpha_{12}$ renders liver more susceptible to fat accumulation.

$G\alpha_{12}$ regulation of SIRT1 contributes to FA oxidation in mitochondria via PPARα network

As an effort to find the molecules regulated by $G\alpha_{12}$ pathway, we performed cDNA microarray analyses using *Gna12* KO liver tissue. First, our analysis of Panther Gene Ontology (GO) term demonstrated that ‘metabolic process’ pathway was notably altered in *Gna12* KO livers (Figure 2A).

Similarly, our additional gene ontology analysis for identical datasets using DAVID bioinformatics program verified that ablation of *Gna12* caused down-regulation of 4 major signaling pathways: DNA metabolism, lipid biosynthesis, amine catabolism, and DNA repair (Figure 2B). Since *Gna12* KO mice did not show obvious growth retardation or any other developmental defects, which may reflect abnormal DNA metabolism (18), we focused on lipid metabolism, particularly alterations in the expression of clusters of genes involved in FA oxidation, with the aim of understanding the basis of altered lipid profiles observed in *Gna12* KO mice. Thorough analysis of the microarray results enabled us to find PPARα target genes as one of the major pathways suppressed by *Gna12* KO (Figure 2C). In the analysis of gene network using STRING database, SIRT1, PPARα and PGC1α as a 'core partners' were found to be closely inter-connected with a subset of genes affected by *Gna12* deficiency (Figure 2D). Of those linked to the core network, the genes associated with lipid catabolism, acyl-CoA metabolism, ketogenesis, and peroxisomal oxidation processes were all markedly suppressed.

We then narrowed our focus on the regulatory potential of $G\alpha_{12}$ on SIRT1, and found that SIRT1 level was distinctly reduced in liver deficient of $G\alpha_{12}$, whereas other isoforms associated with mitochondrial function (i.e., SIRT3 and SIRT5) were not (or minimally if any) affected (Figure 3A) (19). Similar results were obtained in the experiments using primary hepatocytes (Figure 3B, left). Consistently, infection of HepG2 cells with an adenoviral construct encoding for a constitutively active mutant of $G\alpha_{12}$ (Ad-$G\alpha_{12}$QL) increased SIRT1 level, whereas shRNA-mediated stable knockdown of $G\alpha_{12}$ gene in AML12 cells showed the opposite effect (Figure 3B, middle and right). Carnitine palmitoyl transferase-1 (CPT1) and PGC1α levels were also diminished in the liver or in primary hepatocytes (Figure 3C), indicating that *Gna12* ablation might cause a decrease in mitochondrial lipid oxidation. Among the members existing in the core network controlled by SIRT1, attention was paid to PPARα because it is a transcription factor that globally regulates genes associated with FA oxidation in physiologic situations (20). PPARα target gene transcripts responsible for FA oxidation were substantially down-regulated (Figure 3D), being consistent with the inhibition of SIRT1 and PGC1α. In line with this, the oxygen consumption rate (OCR) in mitochondrial

fractions prepared from the liver tissue (Figure 3E) and palmitate oxidation in primary hepatocytes were also decreased (Figure 3F). Our results corroborate the role of $G\alpha_{12}$ in the regulation of FA oxidation which is controlled by PPARα target gene products in conjunction with SIRT1.

Gna12 ablation suppresses SIRT1 along with enhanced fat accumulation under fasting condition

During the period of calorie restriction or fasting, metabolic adaptations occur in various organs by changing a large subset of genes necessary for maintaining energy homeostasis. Given that SIRT1 is induced in the fasting state as a core regulator of lipid metabolism (21, 22), we examined the effect of *Gna12* ablation on adaptive change in SIRT1 under fasting condition. While fasting of WT animals for 24 h markedly increased SIRT1 and CPT1 levels in the liver, *Gna12* KO completely prevented this effect (Figure 4A). In *Gna12* Het mice, the protein levels were partially diminished, strengthening the functional relevance of $G\alpha_{12}$ signaling in our experimental model (Supplemental Figure 1C). In addition, the fasting-inducible transcript levels of *Acadl* and *Acadm* were diminished in the liver of *Gna12* KO mice (Figure 4B). Moreover, *Gna12* KO lowered basal or fasting-inducible SIRT1 expression in skeletal muscle and brown adipose tissue; although the fasting effect on SIRT1 in white adipose tissue seems to be relatively mild, the inhibitory effect of *Gna12* KO on SIRT1 was also observed in this tissue (Supplemental Figure 2). To further evaluate the regulatory role of $G\alpha_{12}$ in lipid metabolism, WT mice were hydrodynamically injected with a plasmid (50 μg) encoding shRNA-$G\alpha_{12}$ (sh-$G\alpha_{12}$) or shRNA-non-targeting control luciferase (sh-Luci) via the tail vein for knockdown of $G\alpha_{12}$ in the liver (10). As expected, mice injected with sh-$G\alpha_{12}$ plasmid exhibited diminished SIRT1 and CPT1 expression in association with increase of liver TG content upon fasting, compared to mice injected with sh-Luci plasmid (Figure 4, C and D). Next, we employed albumin promoter-driven lentiviral $G\alpha_{12}$ delivery system to validate the link between $G\alpha_{12}$ and SIRT1 and to exclude off-target effects. Enforced expression of $G\alpha_{12}$ specifically in hepatocytes caused recovery of SIRT1 and CPT1 expression in the liver of *Gna12* KO mice under fasting condition (Figure 4E). Similarly, hepatic lipid accumulation in the animals was notably attenuated by the lentiviral gene delivery

(Figure 4F). These results indicate that $G\alpha_{12}$ regulates SIRT1 level, and consequently its downstream molecules responsible for mitochondrial FA oxidation.

HIF-1α-mediated USP22 induction contributes to SIRT1 up-regulation by $G\alpha_{12}$

Nutritional status modulates SIRT1 levels through transcriptional and/or post-translational mechanisms (23). Hepatic NAD^+ and NADH contents reciprocally modulate *SIRT1* transcript levels (24). In our study, however, *Gna12* KO mice showed no changes in *Sirt1* mRNA, NAD^+, and NADH in the liver (Supplemental Figure 3A, and Supplemental Figure 3B, left), raising the idea that $G\alpha_{12}$ may post-translationally regulate SIRT1. Consistently, pyruvate and lactate levels, which affect NAD^+/NADH and SIRT1 de novo synthesis (21), were not changed (Supplemental Figure 3B, right). In an effort to find the molecule(s) responsible for SIRT1 regulation, we checked $G\alpha_{12}$ effect on the stability of SIRT1, and found that Ad-$G\alpha_{12}$QL infection not only attenuated the intensities of ubiquitinated SIRT1, but enhanced SIRT1 stability in HepG2 cells, as fortified by the outcome of an experiment using cycloheximide (Figure 5A). These results support the concept that $G\alpha_{12}$ regulation of SIRT1 may result from modulation of protein ubiquitination.

Based on the report that USP22 deubiquitinates SIRT1 for stabilization (25), we examined whether $G\alpha_{12}$ signaling regulates SIRT1 ubiquitination via USP22. The effect of $G\alpha_{12}$ overexpression on SIRT1 ubiquitination was assessed in HepG2 cells deficient of *USP22* (siRNA knockdown). As expected, *USP22* silencing prevented Ad-$G\alpha_{12}$QL from lowering the intensities of ubiquitinated SIRT1 (Figure 5B). In line with this, *Gna12* KO mice displayed a decrease in *Usp22* mRNA in the liver or primary hepatocytes (Figure 5C), demonstrating that $G\alpha_{12}$ signaling regulates SIRT1 ubiquitination through USP22. To find putative transcription factor(s) for USP22 expression downstream from $G\alpha_{12}$, we next used PROMO analysis program and predicted HIF-1α as a candidate interacting with DNA binding sites located in the promoter region of *Usp22* (Figure 5D). In luciferase reporter assays using a construct containing the –2.2 kb region of *Usp22* and its hypoxia regulatory element mutant constructs, the two DNA binding sites located at –539/-535 bp and –287/-283 bp were

functionally active (Figure 5D). In parallel, Ad-Gα_{12}QL infection augmented SIRT1 level in HepG2 cells, and this event depended on HIF-1α or USP22, as evidenced by the results of siRNA knockdown experiments (Figure 5, E and F). In line with several published reports (26-28), inhibition of RhoA/Rock pathway attenuated Gα_{12} overexpression effect on HIF-1α expression (Figure 5G). Consistently, hepatocyte-specific lentiviral delivery of Gα_{12} in *Gna12* KO mice facilitated up-regulation of HIF-1α, USP22 and SIRT1 in the liver (Figure 5H), as corroborated in the experiments using primary hepatocytes from WT or *Gna12* KO mice subjected to Ad-Gα_{12}QL infection (Figure 5I).

To verify the signaling proposed in this study, we performed a hydrodynamic injection of either human USP22 overexpression plasmid or control vector (mock) into *Gna12* KO mice via tail vein; *Gna12* KO mice injected with USP22 plasmid displayed enhanced SIRT1 expression along with attenuated liver TG accumulation upon fasting, compared to *Gna12* KO mice injected with mock vector (Figure 6, A and B). To strengthen our contention that decreased SIRT1 levels by *Gna12* KO may contribute to hepatic steatosis, we examined SIRT1 overexpression effect on changes in fat accumulation in the liver of *Gna12* KO mice under fasting condition. As expected, *Gna12* KO mice exhibited decreased hepatic SIRT1 and CPT1 levels as compared to WT control under fasting condition, which was reversed by SIRT1 overexpression (Figure 6C). Likewise, hepatic lipid accumulation augmented by *Gna12* KO was significantly attenuated by SIRT1 overexpression (Oil Red O staining of liver sections and hepatic TG assays) (Figure 6D). To confirm the role of SIRT1 in Gα_{12} signaling pathway in vitro, we additionally measured OCR in AML12 cells stably expressing sh-Gα12 or control (sh-Luci); Gα_{12} knockdown notably suppressed mitochondrial OCR (i.e., basal, ATP-linked, and maximal respiration), which returned to control level by SIRT1 overexpression (Figure 6E). Similarly, overexpression of SIRT1 sufficiently rescued the phenotype of *Gna12* KO hepatocytes, as proven by diminished lipid accumulation after palmitate treatment (Supplemental Figure 4A). We additionally attempted to examine the effect of Ad-SIRT1 infection on mitochondrial FA oxidation in *Gna12* KO primary hepatocytes; only a slight increase was found in this experiment presumably due to insufficient SIRT1 overexpression (and CPT1 also) in *Gna12* KO hepatocytes as

compared to WT cells (Supplemental Figure 4B). Taken together, these results provide strong evidence that $G\alpha_{12}$ signaling facilitates USP22 expression through HIF-1α, and the induced USP22 stabilizes SIRT1 protein.

HFD feeding renders Gna12 KO mice highly susceptible to liver steatosis

To understand the role of $G\alpha_{12}$ in energy metabolism in the setting of metabolic excess, we examined $G\alpha_{12}$ levels in the livers of both human subjects with NAFLD and obese animal models. In cohort#1, NAFLD patients with either steatosis or steatohepatitis exhibited apparent, but not statistically significant, decreases in hepatic *GNA12* mRNA levels as compared to those in normal subjects (Figure 7A, left). To strengthen the clinical relevance of our finding, we additionally assessed $G\alpha_{12}$ protein levels using a separate set of human liver specimens with varying degree of hepatic steatosis (cohort#2). Of note, $G\alpha_{12}$ protein levels were markedly lowered in livers of patients having either simple steatosis or NASH as compared to individuals without steatosis (Figure 7A, middle and right). However, *GNA12* mRNA and its protein levels tended to slightly decrease in the liver of HFD-fed mice (Figure 7B, left and upper right). In primary hepatocytes from HFD-fed mice, $G\alpha_{12}$ protein level was notably decreased as compared to ND-fed control (Figure 7B, lower right).

Next, we monitored *Gna12* KO effect on liver steatosis and changes in the expression of genes responsible for FA oxidation. HFD-fed *Gna12* KO mice displayed profound fat accumulation in the liver (Figure 7C). Consistently, hepatic TG contents as well as serum LDL cholesterol levels were significantly elevated (Figure 7D and Table 1). Of note, serum liver enzyme activities (e.g. ALT, AST and LDH) and other serum lipid parameters (e.g. total cholesterol, HDL cholesterol, TG and free FA contents) were rather decreased in HFD-fed *Gna12* KO mice (Table 1), presumably due to decreased production of inflammatory mediators in other cell types (29). In line with this, an additional lipidomic analysis from HFD-fed *Gna12* KO mice showed decreases in ceramide and/or sphingolipid contents in plasma (Supplemental Figure 5), supporting our view that overall inflammatory response diminished in whole-body *Gna12* KO mice. Several lines of evidence clearly demonstrates that JNK pathway plays a role in inflammation, contributing to metabolic disease including obesity and insulin

resistance (30-32). Based on the notion that $G\alpha_{12}$ signaling controls JNK activity (33, 34), we examined whether $G\alpha_{12}$ gene knockdown attenuates palmitate-induced apoptosis. As expected, AML12 cells deficient of $G\alpha_{12}$ (AML12-sh-$G\alpha_{12}$) displayed a significant decrease in cytotoxicity upon palmitate treatment (MTT assays) (Supplemental Figure 6A). In parallel with this, cleaved caspase-3 and phosphorylated JNK levels were lowered (Supplemental Figure 6B, left). Palmitate treatment inhibited Akt phosphorylation (i.e., cell viability marker) to a lesser degree in $G\alpha_{12}$ gene knockdown cells than in control cells (Supplemental Figure 6B, right). These outcomes support the possibility that decreased JNK activity might account for attenuated liver injury in *Gna12* KO mice fed on HFD.

The energy metabolizing capacity in organs is governed by a highly dynamic transcriptional network. Based on our finding from microarray analysis that $G\alpha_{12}$ regulates PPARα target gene network comprising SIRT1 (Figure 2), we measured SIRT1 levels in metabolic tissues from WT and *Gna12* KO mice fed HFD. Hepatic SIRT1 level was markedly lowered in *Gna12* KO mice without significant differences in *Sirt1* mRNA, NAD^+, and NADH contents (Figure 7E, upper and Supplemental Figure 3). The transcript levels of lipid oxidation genes were notably suppressed in the liver of HFD-fed *Gna12* KO mice (Figure 7F, upper), whereas those of lipogenic genes were minimally or moderately enhanced presumably due to adaptive changes (Supplemental Figure 7). Similar results were observed in skeletal muscle and white adipose tissue (Figure 7, E and F, middle and lower), strengthening the concept that a deficiency in $G\alpha_{12}$ exacerbates HFD-induced hepatic steatosis as a consequence of decrease in mitochondrial lipid oxidation.

Gna12 KO does not interfere with glucose metabolism and insulin sensitivity

Since liver steatosis is strongly associated with insulin resistance, which contributes to adverse consequences of metabolic syndrome (2-4), we further assessed glucose tolerance and insulin sensitivity using the animal model to see if $G\alpha_{12}$ also controls glucose metabolism. In glucose- or insulin-tolerance tests, time-courses of blood glucose level were slightly different between HFD-fed *Gna12* KO mice and the corresponding WT mice (Supplemental Figure 8, A and B). In the

hyperinsulinemic-euglycemic clamp experiment, the glucose infusion rate required to maintain euglycemia during the clamp was rather weakly enhanced at early times in HFD-fed *Gna12* KO mice although this trend was lost at later steady state (Supplemental Figure 8C). The glucose production rate in the liver at either basal state or under a clamped condition was not changed in the animals (Supplemental Figure 8D). In addition, there were no differences in whole-body glucose flux comprising glucose uptake, glycolysis, and glycogen synthesis (Supplemental Figure 8E). However, it is noteworthy that *Gna12* KO mice fed HFD exhibited lower fasting glucose with hyperinsulinemia compared to WT mice (Table 1). Based on the recent study demonstrating that JNK activation in pancreatic β cells deregulates glucose-stimulated insulin secretion (35), we hypothesized that $G\alpha_{12}$ gene deletion might affect JNK-dependent signaling pathway in β cells since we used a whole-body gene-ablation model. Therefore, we assessed the effect of $G\alpha_{12}$ overexpression on insulin secretion from Min6 cells (a mouse insulinoma-derived cell line displaying characteristics of pancreatic β cells). As expected, $G\alpha_{12}$ overexpression suppressed insulin secretion with JNK activation, which was prevented by JNK inhibitor treatment (Supplemental Figure 8F). Additionally, we assessed insulin degrading enzyme (IDE) in the liver, where approximately two thirds of circulating insulin is degraded as a physiological process called insulin clearance (36), and found that IDE levels in the liver were not different between genotypes (Supplemental Figure 8, G and H). Together, these results support the idea that suppressed JNK signaling and anti-inflammatory response due to whole-body $G\alpha_{12}$ gene deletion contribute to a mild effect on glucose homeostasis distinctively from deregulation of lipid metabolism.

$G\alpha_{12}$ ablation augments diet-induced obesity due to decreased energy expenditure

Next, we monitored the impact of *Gna12* KO on obesity development and whole-body energy expenditure. WT and *Gna12* KO mice fed normal chow diet (ND) showed no difference in body weight gain (Figure 7A, left, lower lines), and had normal phenotype (data not shown). When maintained on HFD for 16 weeks ad libitum, *Gna12* KO mice developed obesity at an accelerated rate as compared to the WT controls (Figure 8A, left, upper lines). Food intake, fecal output and excreted

fecal lipid were all comparable to each other (Figure 8A, right). Of note, a deficiency in $G\alpha_{12}$ gene fortified the effect of HFD feeding on lean mass and fat mass gains (Figure 8B). In HFD-fed *Gna12* KO mice, epididymal fat weight was increased along with adipocyte enlargement (Figure 8C). In parallel, serum leptin levels were doubled in the animals (Figure 8D).

Next, we measured energy expenditure of HFD-fed *Gna12* KO mice using a monitoring system of animal metabolism. *Gna12* KO mice fed HFD showed decreases in total energy expenditure and total oxygen consumption rate than the corresponding WT controls (Figure 8E, left and Figure 8F). Respiratory quotients were not significantly different between genotypes (Figure 8E, right). Body temperature was markedly lower with no change in locomotor activities in *Gna12* KO mice than WT mice (Figure 8G). In an effort to assess whether brown adipose tissue is involved in lowering body temperature observed in *Gna12* KO mice, we examined levels of uncoupling protein 1 (UCP1), an uncoupling protein responsible for thermogenesis, in the tissues of mice fed either ND or HFD, and found no change in UCP1 expression in the brown adipose tissue despite a compensatory increase in its transcript level (Supplemental Figure 9, A and B). Histologic morphology and tissue weights were comparable between genotypes (Supplemental Figure 9C). These results suggest that UCP1-dependent thermogenesis in brown adipose tissue may have a marginal role in lowering body temperature in the animals. Overall, our results demonstrate that *Gna12* KO mice are more susceptible to diet-induced obesity as a consequence of decrease in energy expenditure.

Adenosine signaling may affect $G\alpha_{12}$ regulation of USP22-SIRT1 axis

Several lines of evidence indicate that adenosine signaling has been clinically implicated as a therapeutic target for various pathophysiologic situations including cardiovascular disease, ischemia-reperfusion, and inflammatory disease (37-41). Adenosine functions as biological ligand through binding to distinct corresponding GPCRs (i.e. A_1, A_{2a}, A_{2b}, and A_3) (37, 41). To assess the possible link between adenosine and $G\alpha_{12}$ signaling, SIRT1 levels were measured in WT or $G\alpha_{12}$-deficient mouse embryonic fibroblasts (MEF) treated with each agonist for the receptors in our supplementary experiment. Interestingly, treatment of WT cells with each agonist notably increased SIRT1 level,

which was abrogated by a deficiency of $G\alpha_{12}$ (Supplemental Figure 10A). Similar outcomes were obtained using AML12 cells stably expressing shRNA directed against $G\alpha_{12}$ (sh-$G\alpha_{12}$) (Supplemental Figure 10B). In addition, primary hepatocytes exposed to each adenosine receptor agonist displayed marked increases of SIRT1 and USP22 (Supplemental Figure 10C).

Adenosine concentrations in the extracellular region vary upon metabolic stimuli. Consistently, fasting significantly enhanced serum adenosine concentrations in mice (Supplemental Figure 10D). No change was observed in the liver homogenates. Thus, elevated circulating adenosine in conjunction with increase of $G\alpha_{12}$ would amplify GPCR-mediated SIRT1 induction to maintain systemic energy homeostasis.

Discussion

$G\alpha_{12}$ belongs to heterotrimeric G proteins that controls various cellular responses including growth, motility, proliferation and transdifferentiation (7-11). So far, the impact of $G\alpha_{12}$ on cellular energy metabolism had not been investigated. Our results revealed the novel role of $G\alpha_{12}$ signaling in mitochondrial respiration for the control of lipid oxidation, and the underlying basis on its regulation of SIRT1 as mediated by HIF-1α-dependent transcriptional induction of USP22. Since $G\alpha_{12}$ and SIRT1 are ubiquitously expressed in most metabolic tissues (6), our results support the notion that $G\alpha_{12}$ signaling plays a role in overall FA metabolism and consequently whole-body energy expenditure.

Moreover, we verified that fasting condition increased the level of $G\alpha_{12}$ in the liver in parallel with fat accumulation and that $G\alpha_{12}$ ablation exacerbated fasting-induced liver steatosis along with a decrease in circulating fat. These findings raised the contention that $G\alpha_{12}$ signaling is essential for metabolic processing of fat in the liver and thus its homeostatic balance between liver and systemic lipid metabolism. Our study also showed that the primary mechanism by which $G\alpha_{12}$ controls lipid metabolism engages SIRT1-PPARα-PGC1α axis, as fortified by the results of cDNA microarray and gene network analyses for WT and *Gna12* KO mouse liver. Our results that a deficiency of $G\alpha_{12}$ gene deregulates PPARα target gene expression and thereby increased susceptibility to fasting-induced liver steatosis with diminished FA oxidation are in line with the previous reports demonstrating a link between SIRT1 and PPARα (42, 43). Considering that multifaceted metabolic adaptations comprising SIRT1 induction are observed under a fasting condition, it is highly likely that hepatic $G\alpha_{12}$ level is enhanced as an adaptive response to fasting. Indeed, our result confirmed the lack of fasting induction of Sirt1 by ablation of $G\alpha_{12}$, and the consequent exacerbation of liver steatosis. By the same token, overexpression of either $G\alpha_{12}$ or SIRT1 in the liver by viral gene transfer reversed these effects. Thus, it is highly likely that $G\alpha_{12}$ regulates lipid metabolism in a SIRT1-dependent pathway.

As an extended effort to verify the proposed molecular basis in obesity models, we further examined the role of $G\alpha_{12}$ in liver steatosis from diet-induced obesity model, and found that HFD-fed

Gna12 KO mice displayed massive lipid accumulation in the liver due to suppression of the genes involved in mitochondrial respiration and FA oxidation downstream of SIRT1. Moreover, such outcomes were verified in other tissues including skeletal muscle and white adipose tissue, strengthening the concept that $G\alpha_{12}$ signaling may be responsible for whole-body energy metabolism. In a previous study, however, a certain amount of $G\alpha_{12}$ was found to be localized in mitochondria, negatively modulating its motility, respiration and membrane potential (12). In addition, active mutants of $G\alpha_{12}$ inhibited phosphorylation of Bcl-2, causing mitochondrial fragmentation and membrane permeabilization (12), which represents distinctive features in comparison to our current findings. Considering the notion that the preservation of functional capacity of healthy mitochondria contributes to homeostatic maintenance of FA oxidation, it is also likely that $G\alpha_{12}$ has distinct functions on mitochondria in a SIRT1-independent pathway in accordance with its subcellular distribution (44, 45). The detailed molecular insight into the role of $G\alpha_{12}$ at mitochondria needs to be further explored.

In our results, $G\alpha_{12}$ expression, particularly protein level, was notably diminished in subjects with either simple steatosis or NASH as compared to those without steatosis. Contrary to the findings from human liver specimens, $G\alpha_{12}$ level in the liver of HFD-fed WT mice rather showed mild decrease than ND-fed control despite a notable decrease in primary hepatocytes. Given that $G\alpha_{12}$ plays a key role in inflammatory and immune responses (29, 46), it is presumed that $G\alpha_{12}$ level might be altered in a subset of non-parenchymal cells (e.g. inflammatory cells or fibroblasts) that reside within inflamed fatty liver. Similarly, our previous study also demonstrates that $G\alpha_{12}$ level was up-regulated in hepatic stellate cells in fibrotic liver (47). Thus, we carefully raise the possibility that the severity of inflammatory response and/or fibrotic change affects $G\alpha_{12}$ in the liver although it is quite challenging to compare the degree of inflammation among different species and/or experimental models.

It is well established that JNK activation contributes to chronic inflammation and consequent metabolic disorders (30-32). In our previous report and others, the $G\alpha_{12}$ pathway activates JNK via

RhoA (33, 34), which may explain diminished overall inflammatory responses as indicated by decreases in liver injury markers (i.e., ALT and AST) and inflammatory lipid mediators (i.e., sphingolipids and ceramides) in whole-body *Gna12* KO mice. Similarly, the levels of pro-inflammatory cytokines (e.g., IL-6 and TNFα) secreted predominantly by inflamed adipose tissue were rather lower in *Gna12* KO mice. Hence, diminished inflammation might cause mild changes, if any, in glucose tolerance distinctly from exacerbation in hepatic steatosis and obesity. Previous studies have provided the pathogenic role of SIRT1 deficiency in insulin resistance and hyperglycemia (48-50). However, our results showed unaltered glucose metabolism and insulin sensitivity in HFD-fed *Gna12* KO mice presumably due to diminished inflammatory response. In addition, our finding that *Gna12* KO mice exhibited hyperinsulinemia together with lowered fasting glucose level might result from suppressed JNK signaling in $G\alpha_{12}$-deficient pancreatic β cells. Also, we do not necessarily exclude the possibility that $G\alpha_{12}$ signaling regulates other pathway(s) affecting glucose metabolism.

The observation that $G\alpha_{12}$ stabilizes SIRT1 by decreasing its ubiquitination supports the hypothesis that $G\alpha_{12}$ post-translationally regulates SIRT1. Persistent activation of JNK1 facilitates SIRT1 degradation (51). Since $G\alpha_{12}$ pathway positively controls JNK activity (34), the effect of $G\alpha_{12}$ on SIRT1 deubiquitination depends on a pathway independent from JNK signaling. USP belongs to the members of the deubiquitinase family, controlling target protein stability via inhibition of ubiquitin-mediated proteosomal degradation. Based on the previous observation that USP22 deubiquitinates SIRT1 for stabilization (25), we were tempted to determine whether $G\alpha_{12}$ regulation of SIRT1 engages USP22. Our results demonstrated for the first time that $G\alpha_{12}$ transcriptionally activates the USP22 gene via HIF-1α, leading to inhibition of ubiquitin-mediated SIRT1 degradation as corroborated by the results of our in vivo and in vitro $G\alpha_{12}$ manipulation experiments.

HIF-1α mediates and coordinates metabolic changes upon hypoxic responses, which would be required for maintenance of cellular energy balance including lipid metabolism (52-54). Our finding shown here demonstrates that $G\alpha_{12}$ promotes HIF-1α-dependent USP22 induction, maintaining SIRT1 level. The data showing a bona fide increase of USP22 by enforced expression of Ad-$G\alpha_{12}$QL in *Gna12* KO primary hepatocytes further strengthen the concept that the ability of $G\alpha_{12}$ to stabilize

SIRT1 relies on HIF1α. Our finding is consistent with the report that hypoxic stimuli increase SIRT1 in a HIF-1α-dependent manner (55). Likewise, transgenic mice with adipose tissue-selective expression of a dominant negative form of HIF-1α showed an impairment in energy expenditure with decreased thermogenesis (53). We also verified the role of RhoA/Rock in the regulation of HIF-1α by $G\alpha_{12}$ (26-28). Overall, the outcomes of our study uncover the new $G\alpha_{12}$ signaling cascade encompassing HIF-1α-driven USP22 expression that affects SIRT1 in response to altered metabolic environments.

Considering that a subset of GPCRs generally form oligomeric complexes with other GPCRs (56), it is quite challenging to define a single GPCR or its corresponding ligand(s) responsible for numerous metabolic events. In the present study, however, we attempted to find possible GPCRs and/or ligands for our proposed mechanism, focusing on adenosine signaling as one of candidates. In a recent study, adenosine signaling contributes to alcohol-induced fatty liver in mice (57), supportive of possible involvement of adenosine signaling in our proposed model. In contrast to our finding, it has been claimed that A_{2b} receptor activation down-regulated CPT1 and PPARα (57), which may be due to differences in experimental design (e.g., agonist treatment time; 30 min-12 h vs. 24 h). Thus, more detailed experiments may be necessary to define the receptor activation and $G\alpha_{12}$ coupling at the molecular level. Our results do not exclude the possibility of other G protein (i.e. G_s or G_i) coupling because each adenosine receptor may also couple to the G proteins (37, 41). Nevertheless, our findings provide evidence that adenosine signaling affects $G\alpha_{12}$-mediated USP22 and SIRT1 axis under different physiological conditions.

In summary, we discovered a new function of $G\alpha_{12}$ signaling in lipid metabolism. Since FA oxidation occurs mainly in mitochondria, the identified $G\alpha_{12}$ signaling pathway may fill the missing link between cell surface receptor activation and mitochondrial fuel oxidation. Moreover, our study identifies the regulatory role of $G\alpha_{12}$ signaling in SIRT1-PPARα pathway, delineating the molecular basis by which $G\alpha_{12}$ regulates SIRT1. The findings provide HIF-1α and USP22 as attractive targets for energy expenditure, which would be utilized to combat against obesity epidemic. Current and

466 future investigation of the function and mechanism of this cascade may offer a new insight into the
467 understanding of energy metabolism, and uncover targets for treating metabolic diseases.
468

Methods

Details of the materials and experimental protocols are provided in the Supplementary Materials and Methods.

Animal Experiments

Animal experiments were conducted under the guidelines of the Institutional Animal Use and Care Committee at Seoul National University. All animals were maintained in a 12 h light/dark cycle and fed ad libitum. Details of the generation of the *Gna12* KO mice used in this study have been described previously (17). Male mice at 6-8 weeks of age, unless otherwise indicated, were used in this study. To minimize environmental differences, mice were housed for at least a week before each experiment. For fasting/refeeding transition model, *Gna12*KO mice and their age-matched WT littermates were fed ad libitum, fasted for 24 h, and refed for 24 h with free access to water. For a diet-induced obesity model, age-matched WT and *Gna12* KO mice were subjected to feeding ad libitum either ND or HFD with 60% kcal fat (D12492, Research Diets) for up to 16 weeks. After sacrifice of animals, tissues were dissected, snap-frozen, and processed for protein and RNA quantification (58).

Statistics

Values are expressed as mean±standard error of mean (SEM). Statistical significance was tested by two-tailed Student's *t* test or 1-way ANOVA with Bonferroni or Least Significant Difference (LSD) multiple comparison procedure where appropriate. Differences were considered significant at $P < 0.05$.

Accession code

Microarray data using liver tissues of each genotypes are deposited in the Gene Expression Omnibus (http://www.ncbi.nim.nih.gov/geo/) under the accession number GSE51694.

Study approval

All animal studies were approved by the institutional review board of the Seoul National University and conducted under the guidelines of the IACUC at Seoul National University. Human NAFLD liver specimens were provided by the University of Kansas Liver Center Tissue Bank between 2010 and 2011 (cohort #1) and Cedars-Sinai Medical Center in 2017 (cohort #2). All of the procured specimens received proper patient consents with approval.

Author contributions

THK and YMY designed the studies, performed the experiments and analyzed the data, and drafted the manuscript. CYH and JHK did the acquisition, and analyzed data. HO and SSK performed the metabolic cage and clamp studies, and CSC analyzed and interpreted the data. BHY and YHC performed HPLC experiments for adenosine measurement. TSP performed lipidomic experiments. CHL and HK provided administrative and material support, or did exploratory experiments. MN, ES, and YJW collected, analyzed and provided human samples and edited manuscript. SGK designed and supervised the studies, analyzed and interpreted the data, wrote the manuscript, and obtained funding.

Acknowledgements

We thank Dr. Melvin I. Simon (California Institute of Technology, Pasadena, CA) for the *Gna12* KO mice and MEF cells, and Dr. Patrick J. Casey (Duke University Medical Center, Durham, NC) for the adenovirus encoding mouse $G\alpha_{12}QL$ (Q229L), and Dr. Richard D. Palmiter (University of Washington, Seattle, WA) for mouse albumin enhancer/promoter (NB) construct, and Dr. Junichi Sadoshima (Rutgers New Jersey Medical School, Newark, NJ) for adenovirus encoding mouse SIRT1. We thank Dr. Yu-Jui Yvonne Wan, Dr. Ekihiro Seki, and Dr. Mazen Noureddin for providing human NAFLD liver samples from University of Kansas Medical Center, Liver Tissue Bank (cohort #1, for YJW) and Division of Digestive and Liver Diseases, Department of Medicine, Comprehensive Transplant Center, Cedars-Sinai Medical Center (cohort #2, for ES and MN). Min6 cells were kindly provided by Dr. Eun Young Park (Mokpo National University, Mokpo, Korea). This research was supported mainly by the National Research Foundation of Korea (NRF) grant funded by the Korea government (NRF-2015R1A2A1A10052663, to SGK). THK was supported partly by Basic Science Research Program of the Ministry of Education (NRF-2018R1A6A3A11048112). YMY was supported partly by Basic Science Research Program of the Ministry of Education (NRF-2014R1A6A3A01054056) and by NIH/National Heart, Lung, and Blood Institute (T32HL134637). ES and MN were supported in part by NIH (R01DK085252). HO and CSC were supported by a grant

from the Korea Health Technology R&D Project through the Korea Health Industry Development Institute (KHIDI) funded by the Ministry for Health and Welfare of Korea (HI14C1135).

References

1. Rui L. Energy metabolism in the liver. *Compr Physiol.* 2014;4(1):177-197.
2. Fabbrini E, et al. Obesity and nonalcoholic fatty liver disease: biochemical, metabolic, and clinical implications. *Hepatology.* 2010;51(2):679-689.
3. Eckel RH, et al. The metabolic syndrome. *Lancet.* 2005;365(9468):1415-1428.
4. Browning JD, and Horton JD. Molecular mediators of hepatic steatosis and liver injury. *J Clin Invest.* 2004;114(2):147-152.
5. Worzfeld T, et al. G(12)/G(13)-mediated signalling in mammalian physiology and disease. *Trends Pharmacol Sci.* 2008;29(11):582-589.
6. Strathmann MP, and Simon MI. G alpha 12 and G alpha 13 subunits define a fourth class of G protein alpha subunits. *Proc Natl Acad Sci USA.* 1991;88(13):5582-5586.
7. Xu N, et al. A mutant alpha subunit of G12 potentiates the eicosanoid pathway and is highly oncogenic in NIH 3T3 cells. *Proc Natl Acad Sci U S A.* 1993;90(14):6741-6745.
8. Chan AM, et al. Expression cDNA cloning of a transforming gene encoding the wild-type G alpha 12 gene product. *Mol Cell Biol.* 1993;13(2):762-768.
9. Kelly P, et al. The G12 family of heterotrimeric G proteins promotes breast cancer invasion and metastasis. *Proc Natl Acad Sci U S A.* 2006;103(21):8173-8178.
10. Yang YM, et al. Galpha12 gep oncogene deregulation of p53-responsive microRNAs promotes epithelial-mesenchymal transition of hepatocellular carcinoma. *Oncogene.* 2015;34(22):2910-2921.
11. Grzelinski M, et al. Critical role of G(alpha)12 and G(alpha)13 for human small cell lung cancer cell proliferation in vitro and tumor growth in vivo. *Clin Cancer Res.* 2010;16(5):1402-1415.
12. Andreeva AV, et al. G alpha12 is targeted to the mitochondria and affects mitochondrial morphology and motility. *Faseb j.* 2008;22(8):2821-2831.
13. Wallace DC. Mitochondria and cancer. *Nat Rev Cancer.* 2012;12(10):685-698.
14. Guarente L. Sirtuins as potential targets for metabolic syndrome. *Nature.* 2006;444(7121):868-874.
15. Imai S, et al. Transcriptional silencing and longevity protein Sir2 is an NAD-dependent histone deacetylase. *Nature.* 2000;403(6771):795-800.
16. Donnelly KL, et al. Sources of fatty acids stored in liver and secreted via lipoproteins in patients with nonalcoholic fatty liver disease. *J Clin Invest.* 2005;115(5):1343-1351.
17. Gu JL, et al. Interaction of G alpha(12) with G alpha(13) and G alpha(q) signaling pathways. *Proc Natl Acad Sci U S A.* 2002;99(14):9352-9357.
18. Mazouzi A, et al. DNA replication stress: causes, resolution and disease. *Exp Cell Res.* 2014;329(1):85-93.
19. Chalkiadaki A, and Guarente L. Sirtuins mediate mammalian metabolic responses to nutrient availability. *Nat Rev Endocrinol.* 2012;8(5):287-296.

569 20. Leone TC, et al. A critical role for the peroxisome proliferator-activated receptor alpha
570 (PPARalpha) in the cellular fasting response: the PPARalpha-null mouse as a model of fatty
571 acid oxidation disorders. *Proc Natl Acad Sci U S A.* 1999;96(13):7473-7478.
572 21. Rodgers JT, et al. Nutrient control of glucose homeostasis through a complex of PGC-1alpha
573 and SIRT1. *Nature.* 2005;434(7029):113-118.
574 22. Vega RB, et al. The coactivator PGC-1 cooperates with peroxisome proliferator-activated
575 receptor alpha in transcriptional control of nuclear genes encoding mitochondrial fatty acid
576 oxidation enzymes. *Mol Cell Biol.* 2000;20(5):1868-1876.
577 23. Brooks CL, and Gu W. How does SIRT1 affect metabolism, senescence and cancer? *Nat*
578 *Rev Cancer.* 2009;9(2):123-128.
579 24. Hayashida S, et al. Fasting promotes the expression of SIRT1, an NAD+ -dependent protein
580 deacetylase, via activation of PPARalpha in mice. *Mol Cell Biochem.* 2010;339(1-2):285-292.
581 25. Lin Z, et al. USP22 antagonizes p53 transcriptional activation by deubiquitinating Sirt1 to
582 suppress cell apoptosis and is required for mouse embryonic development. *Mol Cell.*
583 2012;46(4):484-494.
584 26. Turcotte S, et al. HIF-1alpha mRNA and protein upregulation involves Rho GTPase
585 expression during hypoxia in renal cell carcinoma. *J Cell Sci.* 2003;116(Pt 11):2247-2260.
586 27. Hayashi M, et al. Hypoxia up-regulates hypoxia-inducible factor-1alpha expression through
587 RhoA activation in trophoblast cells. *J Clin Endocrinol Metab.* 2005;90(3):1712-1719.
588 28. Ohta T, et al. Inhibition of the Rho/ROCK pathway enhances the efficacy of cisplatin through
589 the blockage of hypoxia-inducible factor-1alpha in human ovarian cancer cells. *Cancer Biol*
590 *Ther.* 2012;13(1):25-33.
591 29. Ki SH, et al. Galpha12 specifically regulates COX-2 induction by sphingosine 1-phosphate.
592 Role for JNK-dependent ubiquitination and degradation of IkappaBalpha. *J Biol Chem.*
593 2007;282(3):1938-1947.
594 30. Vallerie SN, and Hotamisligil GS. The role of JNK proteins in metabolism. *Sci Transl Med.*
595 2010;2(60):60rv65.
596 31. Hirosumi J, et al. A central role for JNK in obesity and insulin resistance. *Nature.*
597 2002;420(6913):333-336.
598 32. Shoelson SE, et al. Inflammation and insulin resistance. *J Clin Invest.* 2006;116(7):1793-1801.
599 33. Nagao M, et al. The Src family tyrosine kinase is involved in Rho-dependent activation of c-
600 Jun N-terminal kinase by Galpha12. *Oncogene.* 1999;18(31):4425-4434.
601 34. Cho MK, et al. Role of Galpha12 and Galpha13 as novel switches for the activity of Nrf2, a
602 key antioxidative transcription factor. *Mol Cell Biol.* 2007;27(17):6195-6208.
603 35. Lanuza-Masdeu J, et al. In vivo JNK activation in pancreatic beta-cells leads to glucose
604 intolerance caused by insulin resistance in pancreas. *Diabetes.* 2013;62(7):2308-2317.
605 36. Tokarz VL, et al. The cell biology of systemic insulin function. *J Cell Biol.* 2018.
606 37. Hasko G, et al. Adenosine receptors: therapeutic aspects for inflammatory and immune
607 diseases. *Nat Rev Drug Discov.* 2008;7(9):759-770.

608 38. Eltzschig HK, et al. Purinergic signaling during inflammation. *N Engl J Med.*
609 2012;367(24):2322-2333.
610 39. Eltzschig HK, and Carmeliet P. Hypoxia and inflammation. *N Engl J Med.* 2011;364(7):656-
611 665.
612 40. Eltzschig HK, and Eckle T. Ischemia and reperfusion--from mechanism to translation. *Nat*
613 *Med.* 2011;17(11):1391-1401.
614 41. Chen JF, et al. Adenosine receptors as drug targets--what are the challenges? *Nat Rev Drug*
615 *Discov.* 2013;12(4):265-286.
616 42. Purushotham A, et al. Hepatocyte-specific deletion of SIRT1 alters fatty acid metabolism and
617 results in hepatic steatosis and inflammation. *Cell Metab.* 2009;9(4):327-338.
618 43. Li Y, et al. Hepatic SIRT1 attenuates hepatic steatosis and controls energy balance in mice
619 by inducing fibroblast growth factor 21. *Gastroenterology.* 2014;146(2):539-549.e537.
620 44. Hampoelz B, and Knoblich JA. Heterotrimeric G proteins: new tricks for an old dog. *Cell.*
621 2004;119(4):453-456.
622 45. Chisari M, et al. Shuttling of G protein subunits between the plasma membrane and
623 intracellular membranes. *J Biol Chem.* 2007;282(33):24092-24098.
624 46. Won HY, et al. Galpha12 is critical for TCR-induced IL-2 production and differentiation of T
625 helper 2 and T helper 17 cells. *Biochem Biophys Res Commun.* 2010;394(3):811-816.
626 47. Kim KM, et al. Galpha12 overexpression induced by miR-16 dysregulation contributes to liver
627 fibrosis by promoting autophagy in hepatic stellate cells. *J Hepatol.* 2018;68(3):493-504.
628 48. Wang RH, et al. Hepatic Sirt1 deficiency in mice impairs mTorc2/Akt signaling and results in
629 hyperglycemia, oxidative damage, and insulin resistance. *J Clin Invest.* 2011;121(11):4477-
630 4490.
631 49. Purushotham A, et al. Systemic SIRT1 insufficiency results in disruption of energy
632 homeostasis and steroid hormone metabolism upon high-fat-diet feeding. *Faseb j.*
633 2012;26(2):656-667.
634 50. Schenk S, et al. Sirt1 enhances skeletal muscle insulin sensitivity in mice during caloric
635 restriction. *J Clin Invest.* 2011;121(11):4281-4288.
636 51. Gao Z, et al. Sirtuin 1 (SIRT1) protein degradation in response to persistent c-Jun N-terminal
637 kinase 1 (JNK1) activation contributes to hepatic steatosis in obesity. *J Biol Chem.*
638 2011;286(25):22227-22234.
639 52. Nishiyama Y, et al. HIF-1alpha induction suppresses excessive lipid accumulation in alcoholic
640 fatty liver in mice. *J Hepatol.* 2012;56(2):441-447.
641 53. Zhang X, et al. Adipose tissue-specific inhibition of hypoxia-inducible factor 1{alpha} induces
642 obesity and glucose intolerance by impeding energy expenditure in mice. *J Biol Chem.*
643 2010;285(43):32869-32877.
644 54. Wilson GK, et al. Hypoxia inducible factors in liver disease and hepatocellular carcinoma:
645 current understanding and future directions. *J Hepatol.* 2014;61(6):1397-1406.
646 55. Chen R, et al. Hypoxia increases sirtuin 1 expression in a hypoxia-inducible factor-dependent

manner. *J Biol Chem.* 2011;286(16):13869-13878.

56. Palczewski K. Oligomeric forms of G protein-coupled receptors (GPCRs). *Trends Biochem Sci.* 2010;35(11):595-600.

57. Peng Z, et al. Adenosine signaling contributes to ethanol-induced fatty liver in mice. *J Clin Invest.* 2009;119(3):582-594.

58. Kim TH, et al. An active metabolite of oltipraz (M2) increases mitochondrial fuel oxidation and inhibits lipogenesis in the liver by dually activating AMPK. *Br J Pharmacol.* 2013;168(7):1647-1661.

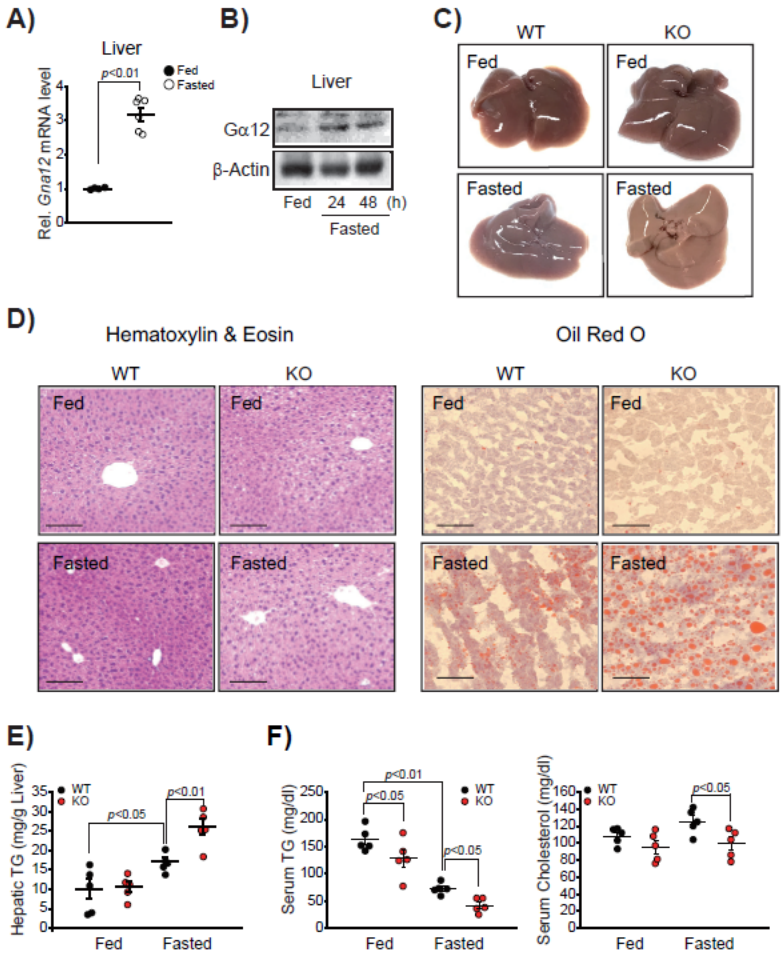

Fig. 1

Figure 1. Association of Gα$_{12}$ signaling with fasting-induced liver steatosis

(**A**) qRT-PCR assays for *Gna12* in the liver from 10-week-old mice fed ad libitum or fasted for 24 h (n = 4-6/group).

(**B**) Immunoblotting for Gα$_{12}$ in liver homogenates from WT mice fed normal chow diet ad libitum or fasted for indicated times. The blots were run in parallel using same samples.

(**C**) Representative gross appearance of liver tissues from the mice as in **A** (n=3/group).

(**D**) Representative H&E staining (left; n=5/group) and Oil Red O staining (right; n=3/group) of the liver sections. Scale bar, 100 μm

(**E**) Hepatic triglyceride (TG) contents (n=5/group).

(**F**) Serum TG and total cholesterol levels (n=5/group).

Values represent the mean ± SEM. Data were analyzed by two-tailed Student's *t* test (**A**) or ANOVA followed by LSD post hoc tests (**E** and **F**).

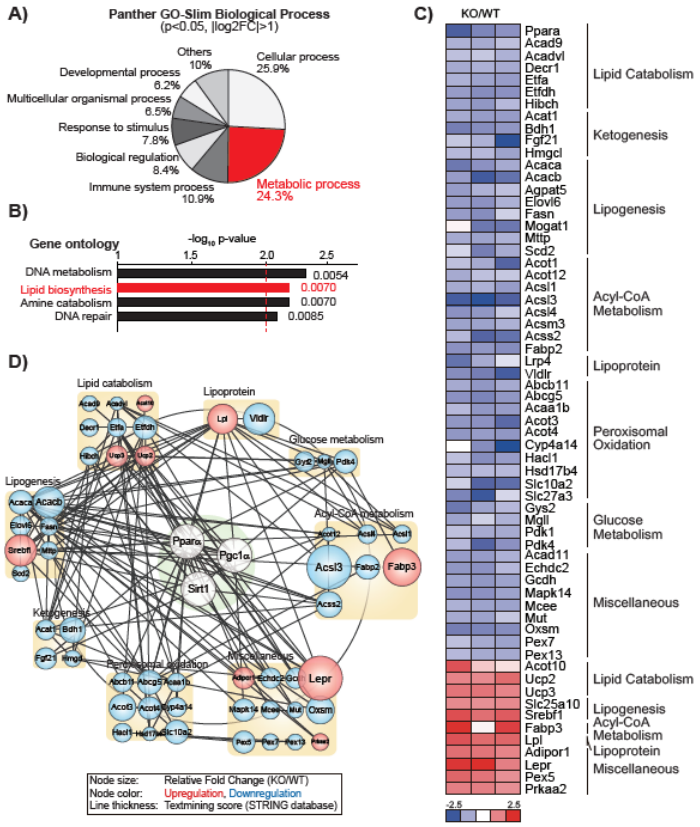

Fig. 2

Figure 2. Gα_{12} regulation of mitochondrial respiration via SIRT1-PPARα network

(**A**) PANTHER pathway analysis in the cDNA microarrays performed using RNA samples extracted from the liver of 8-week-old male WT or *Gna12* KO mice that had been fasted overnight before sacrifice (n=3/group). % represents the percentage of the number of genes that belong to respective pathway categories over total number of genes analyzed.

(**B**) Gene ontology analysis of major signaling pathways in the cDNA microarrays using DAVID bioinformatics database.

(**C**) Heat map of the genes associated with energy metabolism in the same cDNA microarrays used in **A**. The $\log_2$ ratios of *Gna12* KO/WT were presented using heat map (blue, under-expression; and red, over-expression).

(**D**) Core network analysis associated with the SIRT1-PPARα pathway. PPARα-associated genes affected by *Gna12* KO are represented as colored circles and assigned to specific sub-categories. Genes up-regulated (red circles) or down-regulated (blue circles) in the microarrays were shown for each sub-category. Line thickness represents the strength of evidence provided by the STRING database.

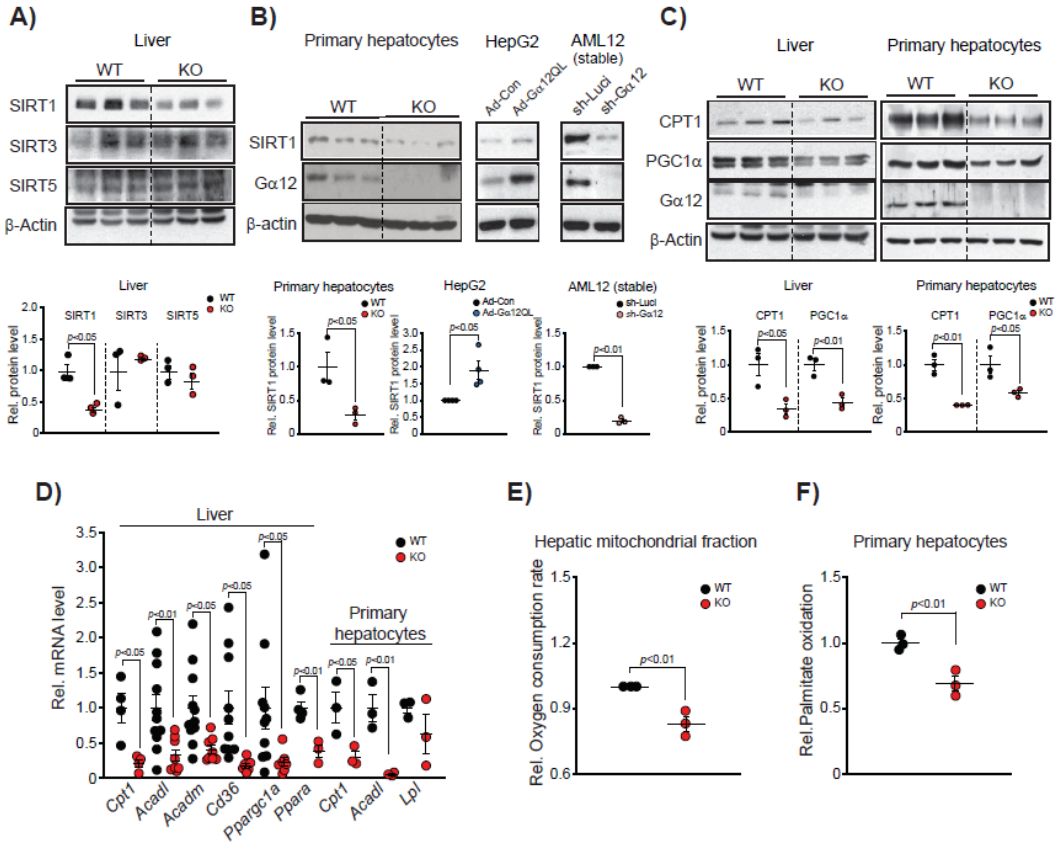

Fig. 3

Figure 3. Gα$_{12}$ regulation of SIRT1-dependent mitochondrial respiration in the liver

(**A**) SIRT1 inhibition by *Gna12* KO. Immunoblottings for SIRT1, SIRT3 and SIRT5 were performed using the liver homogenates from 14-week-old WT or *Gna12* KO mice fed ND (upper), and were quantified (lower, n=3/group).

(**B**) The effects of Gα$_{12}$ modulations on SIRT1 level. Immunoblottings for SIRT1 were done (upper) and quantified (lower) using primary hepatocytes from WT or *Gna12* KO mice (left, n=3/group), HepG2 cells infected with Ad-Gα$_{12}$QL or control (Ad-Con) (middle, n=4/group), or AML12 cells stably expressing sh-Gα$_{12}$ or control (sh-Luci) (right, n=3/group).

(**C**) Immunoblottings for CPT1 and PGC1α in liver or primary hepatocytes from WT or *Gna12* KO mice (upper), and their respective quantifications (lower, n=3/group each).

(**D**) qRT-PCR assays for PPARα target genes responsible for FA oxidation in the liver or primary hepatocytes (n=3-11/group).

(**E**) Oxygen consumption rate in mitochondria. The oxygen consumption rate (OCR) was measured using the mitochondrial fraction prepared from the liver tissues of WT or *Gna12* KO mice (n=3/group). Analyzed OCR was normalized to the protein concentrations for each set of samples

706 determined by the Bradford method.
707 (**F**) Palmitate oxidation in primary hepatocytes. The [^{3}H]-palmitate oxidation rate was determined
708 using primary hepatocytes from WT or *Gna12* KO mice. 5×10^{5} cells per well were cultured in 12-well
709 plates. Data shown is from one representative experiment of two independent experiments (n=3
710 mice/group). Each dot represents an individual pool of primary hepatocytes isolated from each mouse.
711 Values represent mean ± SEM. Data were analyzed by two-tailed Student's *t* test (**A**-**F**). For **A**-**C**, the
712 blots in each panel were run in parallel using same samples and β-actin was used as a normalization
713 control for densitometric analysis.
714

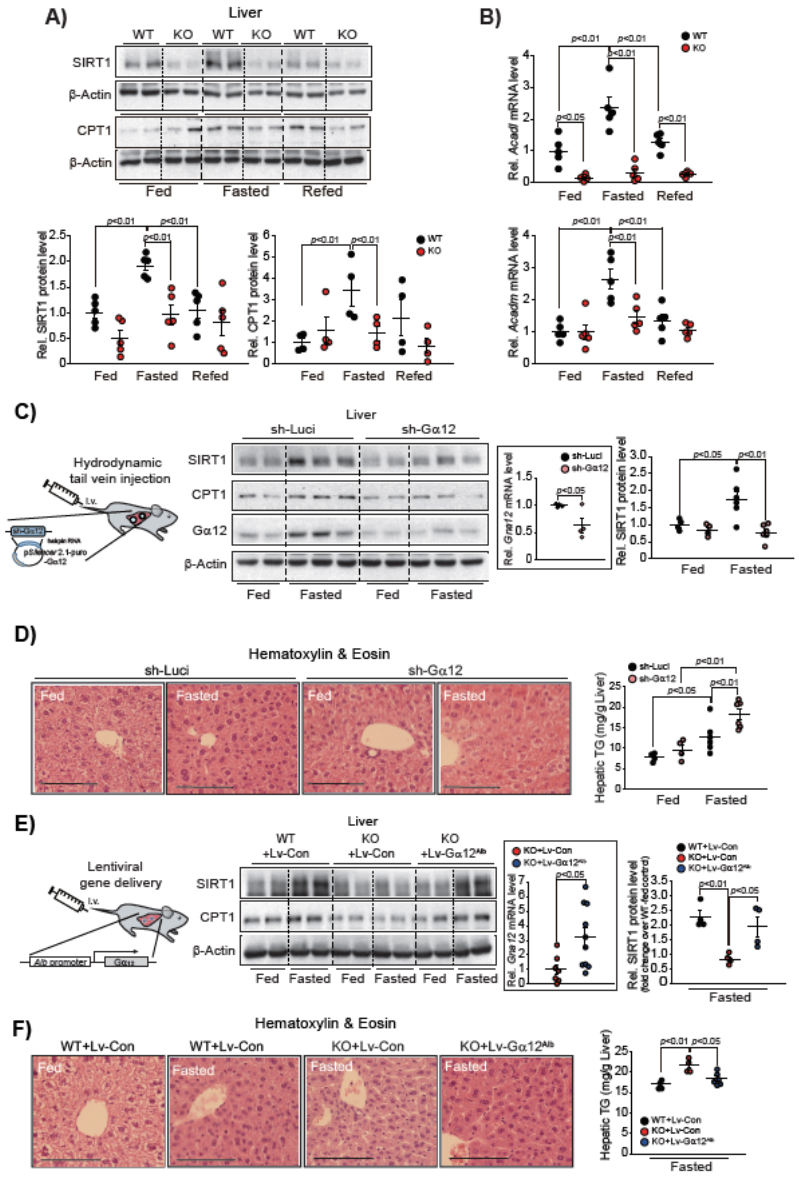

Fig. 4

Figure 4. Lack of fasting induction of SIRT1 by *Gna12* KO

(**A**) Abrogation of SIRT1 and CPT1 induction upon fasting by *Gna12* KO. Immunoblottings for SIRT1 and CPT1 were done and quantified on the liver homogenates from 12-week-old mice fed ad libitum, followed by fasting and re-feeding for 24 h (n=4-5/group).

(**B**) qRT-PCR assays for *Acadl* and *Acadm* in the liver (n=5/group).

(**C**) The effect of hepatic $G\alpha_{12}$ gene knockdown on fasting induction of SIRT1. Immunoblottings for SIRT1 and CPT1 (left) in the liver homogenates, and SIRT1 quantification (right). Mice at 8 weeks of age were subjected to hydrodynamic injection with the plasmid expressing sh-$G\alpha_{12}$ or control (sh-Luci) (n=4-6/group). Inset, qRT-PCR assay for *Gna12* in the liver (n=4/group).

(**D**) Representative H&E staining (left), and hepatic triglyceride (TG) contents (right) from the same

mice as in **C** (n=4-6/group). Scale bar, 100 μm

(**E**) The effect of hepatocyte-specific $G\alpha_{12}$ overexpression on fasting induction of SIRT1. Immunoblottings for SIRT1 and CPT1 were done on the liver homogenates from 8-week-old WT or *Gna12* KO mice injected with Lv-$G\alpha12^{alb}$ (or control) (left), and SIRT1 quantification (right). The mice were subjected to fasting as in **A**. (n=4/group). Inset, qRT-PCR assay for *Gna12* in the liver (n=7-10/group).

(**F**) Representative H&E staining (left), and hepatic TG contents (right) from mice as described in **E** (n=4-6/group). For **E** and **F**, only fasted groups were analyzed for ease of data presentation. Scale bar, 100 μm

Values represent the mean ± SEM. Data were analyzed by two-tailed Student's *t* test (**C** and **E**, insets) or ANOVA followed by LSD (**A** and **D**) or Bonferroni (**B**, **C**, **E** and **F**) post hoc tests. For **A, C** and **E**, the blots in each panel were run in parallel using same samples and β-actin was used as a normalization control for densitometric analysis.

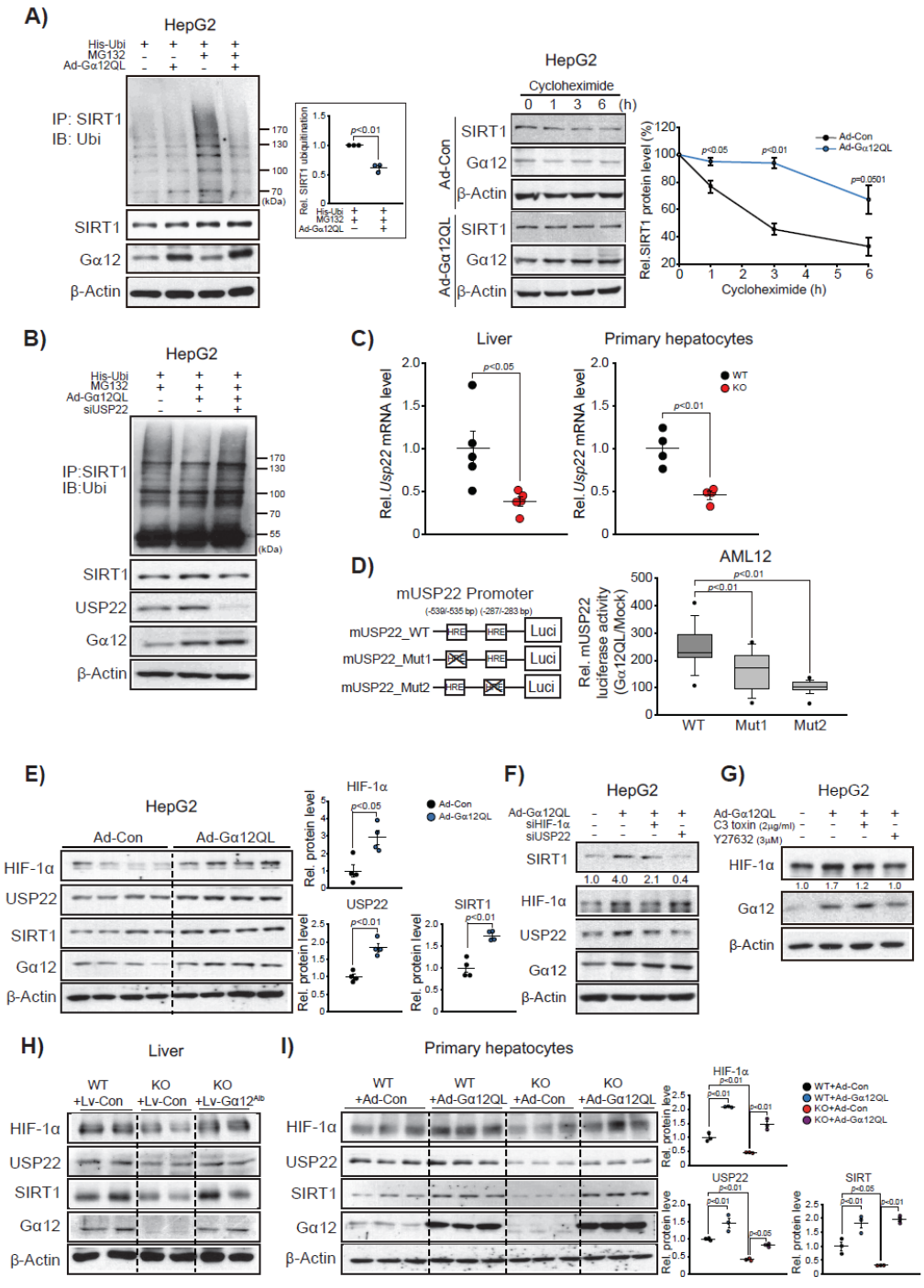

Fig.5

Figure 5. Gα$_{12}$ regulation of SIRT1 via HIF-1α-mediated induction of USP22

(**A**) Inhibition of SIRT1 ubiquitination and degradation by Gα$_{12}$. SIRT1 immunoprecipitates from HepG2 cells infected with Ad-Gα$_{12}$QL (or Ad-Con) were immunoblotted for ubiquitin (left), and quantified (inset, n=3). In another experiment, HepG2 cells were treated with 10 μM cycloheximide for indicated times (right, n=3).

(**B**) The effect of USP22 gene silencing on inhibition of SIRT1 ubiquitination by $G\alpha_{12}$.

(**C**) qRT-PCR assays for *Usp22* in the liver (left, n=5/group) or primary hepatocytes (right, n=4/group).

(**D**) Luciferase reporter assays for USP22 promoter activity in $G\alpha_{12}$-overexpressed AML12 cells. The result shown is combined from three independent experiments (n=6-8 replicates/group for each experiment). Box-and-whisker plot shows median (horizontal lines within boxes), 5-95% percentile (the bounds of the boxes), and range of minimum to maximum values (whiskers). Each dot represents an outlying value. Mut1 or Mut2, promoter-reporter constructs with deletion of respective HIF-1α response element sites.

(**E**) Increase in SIRT1 level by $G\alpha_{12}$ overexpression through HIF-1α-USP22 axis (right, n=4/group).

(**F**) The effect of HIF-1α or USP22 gene silencing on SIRT1 induction by $G\alpha_{12}$.

(**G**) The effect of RhoA/Rock pathway inhibition on HIF-1α induction by $G\alpha_{12}$.

(**H**) The effect of $G\alpha_{12}$ overexpression in the liver on HIF-1α-USP22-SIRT1 axis. Immunoblottings were done on the liver homogenates obtained from mice as in Figure 4E.

(**I**) The effect of $G\alpha_{12}$ overexpression in hepatocytes on HIF-1α-USP22-SIRT1 axis. Immunoblottings were done on mouse primary hepatocytes infected with Ad-$G\alpha_{12}$QL (or Ad-Con) and quantified respectively (n=3/group).

Values represent the mean ± SEM. Data were analyzed by two-tailed Student's *t* test (**A**, **C**, **D** and **E**) or ANOVA followed by Bonferroni post hoc test (**I**). For **A**, **B**, and **E-I**, the blots in each panel were run in parallel using same samples and β-actin was used as a normalization control for densitometric analysis.

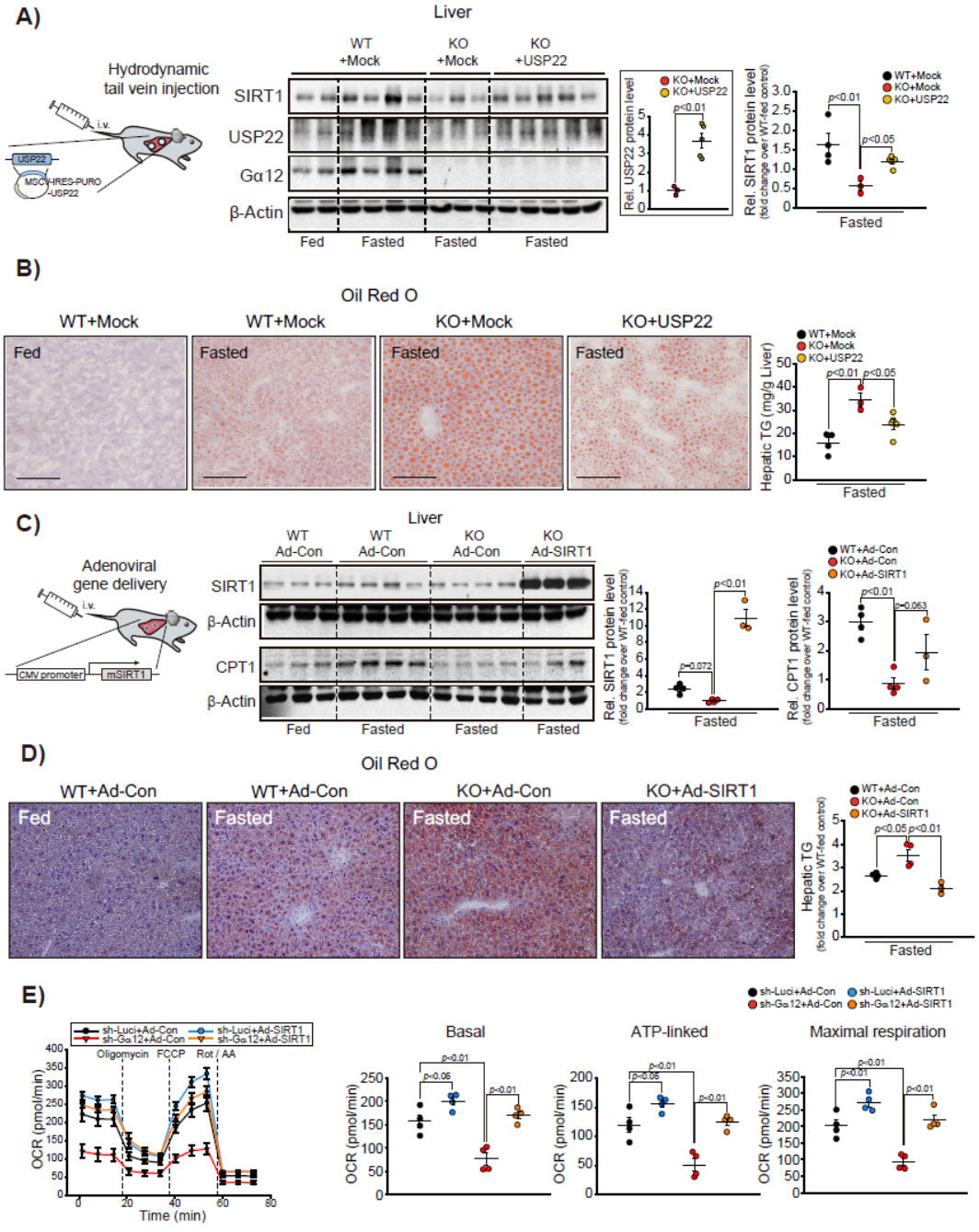

Fig.6

Figure 6. Rescue of metabolic phenotype of *Gna12* KO by overexpression of USP22 or SIRT1

(**A**) The effect of hepatic USP22 overexpression on SIRT1 induction by fasting. Immunoblotting for SIRT1 and USP22 (left) in the liver homogenates, and SIRT1 quantification (right). WT and *Gna12* KO mice at 12 weeks of age were hydrodynamically injected with the plasmid expressing USP22 or control vector (Mock) (n=3-5/group). Inset, densitometric analysis for USP22 in the liver (n=3-5/group).

(**B**) Representative Oil Red O staining (left), and hepatic triglyceride (TG) contents (right) (n=3-

5/group). Scale bar, 100 μm

(**C**) The effect of hepatic SIRT1 overexpression on CPT1 induction by fasting. Immunoblotting for SIRT1 and CPT1 (left) in the liver homogenates, and their respective quantifications (right) (n=3-4/group). WT and *Gna12* KO mice at 15 weeks of age were injected with the adenovirus carrying mouse SIRT1 (Ad-SIRT1, 2.8×10^9 PFU/mouse) or GFP control (Ad-Con).

(**D**) Representative Oil Red O staining (left, original magnification ×20), and TG contents (right) in the liver tissues (n=3-4/group).

(**E**) The effect of SIRT1 overexpression on oxygen consumption rate (OCR) in AML12 cells. OCR was measured in AML12-sh-$G\alpha_{12}$ (or AML12-sh-Luci) cells infected with Ad-SIRT1 (or Ad-Con) in the presence of oligomycin (1 μM), FCCP (1 μM), or rotenone plus antimycin A (0.5 μM each). The results represent four independent experiments (n=6-8 replicates/group for each experiment).

Values represent the mean ± SEM. Data were analyzed by two-tailed Student's *t* test (**A**, inset) or ANOVA followed by LSD (**A**, **C**, and **E**) or Bonferroni (**B** and **D**) post hoc tests. For **A-D**, only fasted groups were analyzed for ease of data presentation. For **A** and **C**, the blots in each panel were run in parallel using same samples and β-actin was used as a normalization control for densitometric analysis.

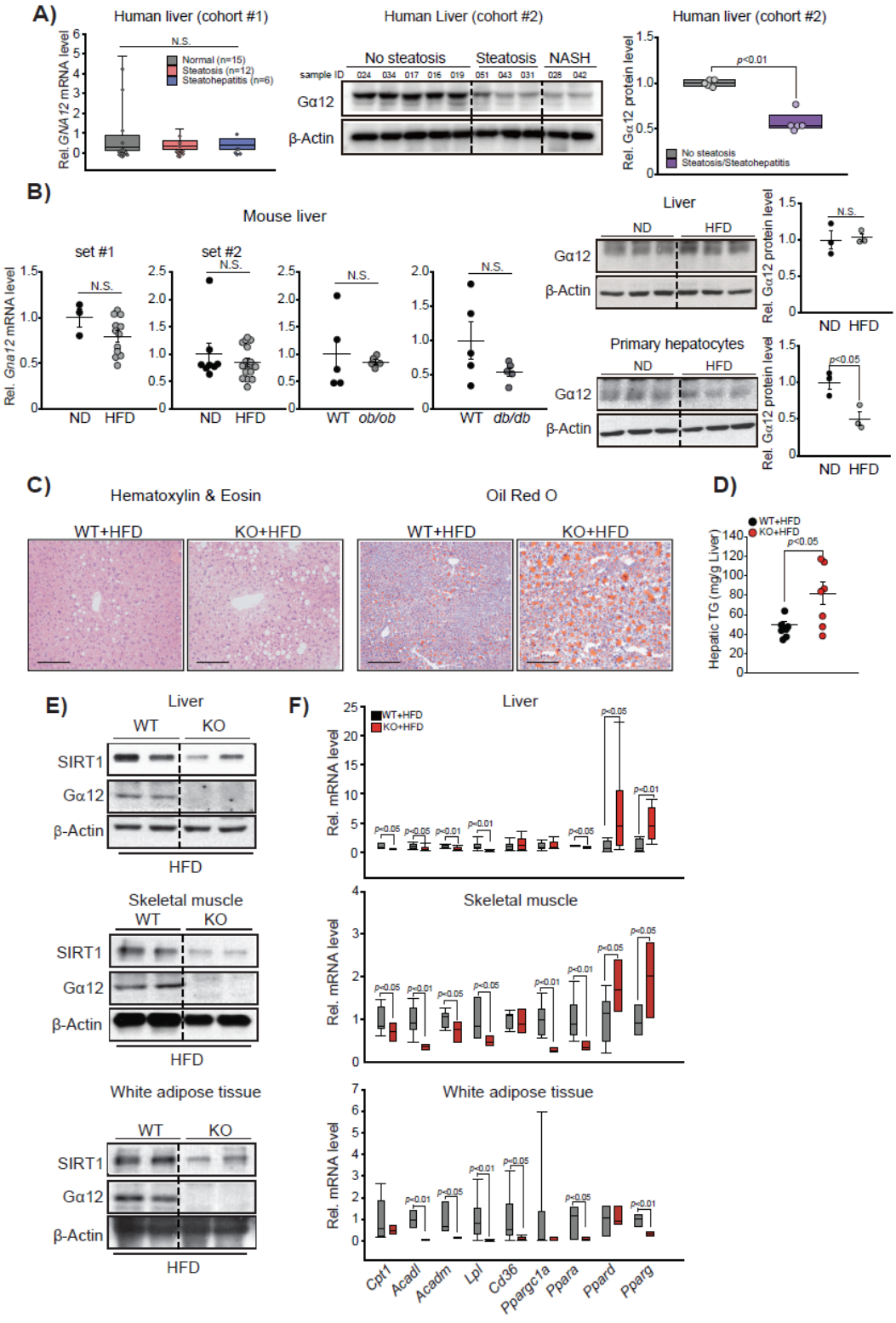

Fig. 7

Figure 7. Augmented liver steatosis and decreased FA oxidation in *Gna12* KO mice fed HFD

(**A**) qRT-PCR assays for *GNA12* (left, n=6-15/group for cohort #1), immunoblotting for $G\alpha_{12}$ (middle, n=2-5/group for cohort #2), and quantification of $G\alpha_{12}$ levels (right, cohort #2) in human liver specimens obtained from NAFLD patients or normal subjects. Each dot represents an individual

subject.

(**B**) qRT-PCR assays and immunoblottings for $G\alpha_{12}$ in mouse liver. *Gna12* mRNA levels were analyzed in the liver of mice fed HFD (or ND) for 8 weeks (n=3 or 12/group for set #1) or 9 weeks (n=8 or 16/group for set #2), or *ob*/*ob* or *db*/*db* mice (n=5/group). For immunoblottings, $G\alpha_{12}$ levels were assessed in the liver or primary hepatocytes from mice as in set #2 and quantified respectively (n=3/group).

(**C**) Representative H&E staining (left) or Oil red O (right) staining of the liver tissue from WT or *Gna12* KO mice fed HFD for 16 weeks (n=3/group). Scale bar, 100 μm

(**D**) Hepatic triglycerides (TG) contents in WT or *Gna12* KO mice as in **C** (n=7/group).

(**E**) Immunoblottings for SIRT1 in the liver (upper), skeletal muscle (middle), or white adipose tissue (lower) from the same mice as in **C**.

(**F**) qRT-PCR assays for transcripts associated with FA oxidation in the liver (n=6-14/group), skeletal muscle (n=6-10/group), or white adipose tissue (n=4-12/group) from the same mice as in **C**.

Values represent the mean ± SEM. Data were analyzed by two-tailed Student's *t* test (**A**, **B**, **D** and **F**). For **A**, **B** and **E**, the blots were run in parallel using same samples and β-actin was used as a normalization control for densitometric analysis. For **A** and **F**, box-and-whisker plots show median (horizontal lines within boxes), 5-95% percentile (the bounds of the boxes), and range of minimum to maximum values (whiskers). N.S., not significant

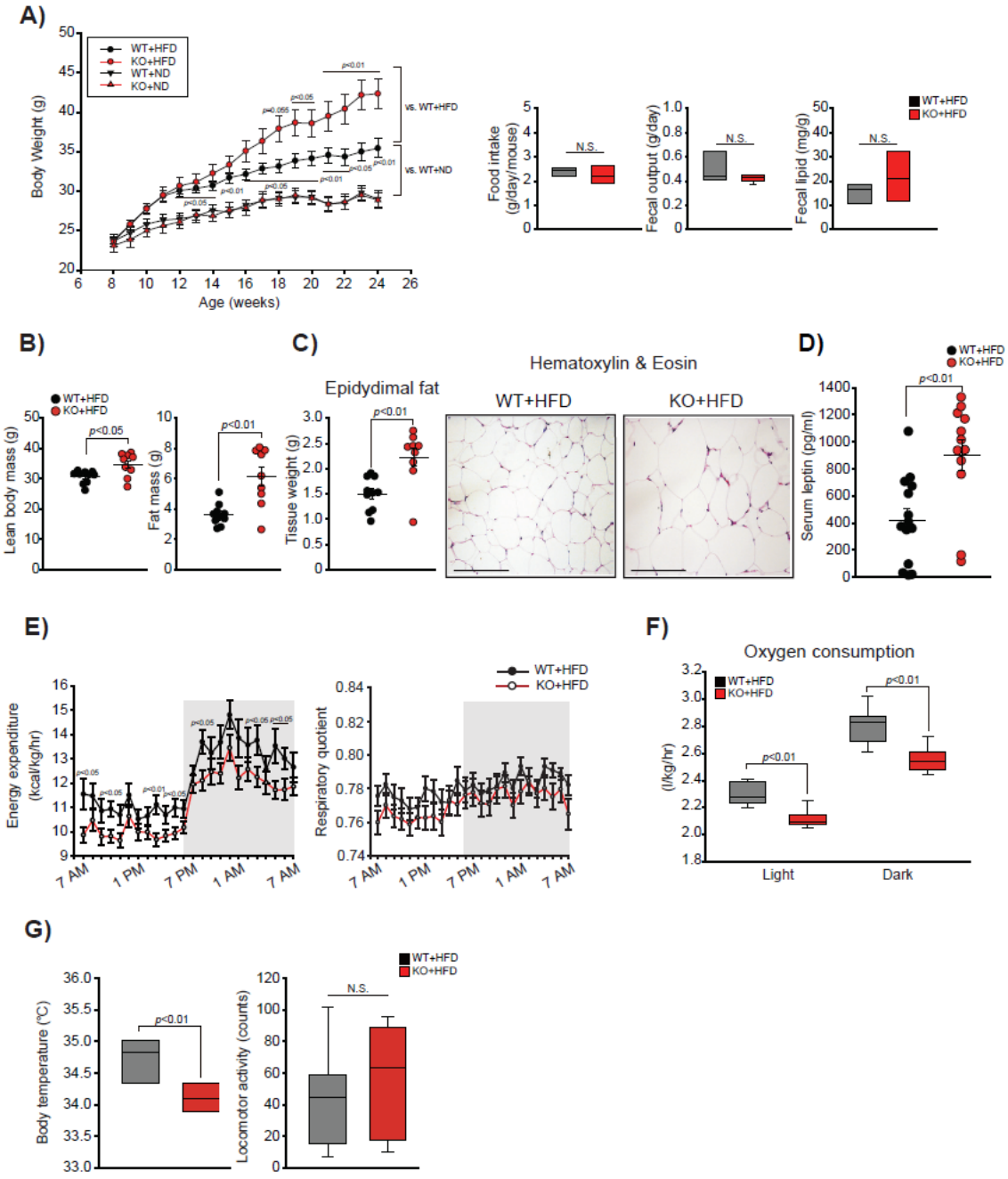

Fig. 8

Figure 8. Changes in whole-body energy metabolism and adiposity by a deficiency of $G\alpha_{12}$

(**A**) The effect of *Gna12* KO on body weight gains, food intake, fecal output and fecal lipid content in mice fed HFD. Body weight (n=8-14/group) and daily food intake (n=9-10/group) of WT or *Gna12* KO mice fed HFD were monitored once every week for 16 weeks. Fecal output and fecal lipid content were measured during the 13th week (n=9-10/group).

(**B**) Adiposity in *Gna12* KO mice fed HFD. Fat mass was assessed by weighing total epididymal, mesenteric, inguinal, perirenal fat pads, and brown adipose tissue. The lean body mass was assessed

by subtracting fat mass from total body mass (left, n=9-10/group).

(**C**) Epididymal fat pad weight (left, n=9-10/group) and representative H&E staining (right, n=3/group) of white adipose tissue from WT or *Gna12* KO mice fed HFD for 16 weeks. Scale bar, 100 μm

(**D**) ELISA assays for serum leptin (n=12-14/group).

(**E**) Energy expenditure and respiratory quotient profiles. The metabolic profiles were measured in WT or *Gna12* KO mice fed HFD for 4 weeks using comprehensive animal metabolic monitoring system (CLAMS) (n=11- 12/group).

(**F**) Whole-body oxygen consumption. Oxygen consumption was measured in mice as described in **E** (n=11-12/group).

(**G**) Body temperature and locomotor activity. Resting rectal body temperature was measured in WT or *Gna12* KO mice fed HFD for 12 weeks (left, n=5-6/group). Locomotor activities were monitored using CLAMS in mice as described in **E** (right, n=11- 12/group).

Values represent the mean ± SEM. Data were analyzed by ANOVA followed by Bonferroni (**A**) post hoc test or two-tailed Student's *t* test (**B**-**F**). For **A**, **F** and **G**, box-and-whisker plots show median (horizontal lines within boxes), 5-95% percentile (the bounds of the boxes), and range of minimum to maximum values (whiskers). N.S., not significant

853 Table 1. The serum metabolic profiles in WT and *Gna12* KO mice fed either ND or HFD for 16

854 weeks.

	HFD		ND	
	WT	*Gna12* KO	WT	*Gna12* KO
ALT (U/l)	79.7 ± 3.5**	60.3 ± 4.2**,##	43.2 ± 2.1	38.8 ± 2.0
AST (U/l)	278.3 ± 25.8*	183.1 ± 8.9**,##	176.8 ± 10.6	132.0 ± 6.8#
LDH (U/l)	2631.4 ± 148.4**	1862. 6 ± 81.3**,##	1180.3 ± 96.9	1192.3 ± 154.6
Fasting glucose (mg/dl)	168.4 ± 4.3**	131.3 ± 3.3**,##	70.0 ± 5.5	65.8 ± 4.3
Insulin (ng/ml)	0.74 ± 0.13**	1.68 ± 0.20**,##	0.20 ± 0.02	0.17 ± 0.07
C-peptide (pM)	359.7 ± 48.9*	602.7 ± 43.8**,##	213.4 ± 39.2	273.1 ± 48.0
Resistin (ng/ml)	2.87 ± 0.14*	3.23 ± 0.28*	2.34 ± 0.14	2.41 ± 0.20
Total adiponectin (μg/ml)	12.43 ± 0.75**	19.70 ± 0.81##	16.82 ± 1.01	18.15 ± 1.38
HMW adiponectin (μg/ml)	3.42 ± 0.31	5.54 ± 0.57##	3.93 ± 0.46	4.94 ± 0.52
IL-6 (pg/ml)	20.7 ± 1.5	17.8 ± 0.5**	22.1 ± 1.0	24.8 ± 2.6
TNFα (pg/ml)	11.3 ± 1.8*	10.4 ± 2.5*	5.3 ± 1.9	4.0 ± 1.0
Total cholesterol (mg/dl)	150.9 ± 3.0**	122.8 ± 4.2##	117.8 ± 6.1	116.5 ± 4.1
HDL cholesterol (mg/dl)	98.4 ± 1.8**	72.2 ± 2.4##	75.3 ± 4.6	64.7 ± 4.9
LDL cholesterol (mg/dl)	8.0 ± 0.2**	10.3 ± 0.8#	6.4 ± 0.4	10.3 ± 1.6#
Triglyceride (mg/dl)	88.9 ± 2.6**	66.0 ± 2.2##	73.0 ± 3.5	65.3 ± 5.4
Free fatty acids (μEq/l)	1022.2 ± 27.3**	845.7 ± 35.8**,##	1322.2 ± 94.7	1274.3 ± 26.2

855

856 Values are presented as the mean±SEM (n=3-14/group).

857 *P<0.05, **P<0.01 vs. significant compared with the respective ND

858 #P<0.05, ##P<0.01 vs. significant compared with the respective WT

859